

Giant oscillating magnetoresistance in silicene-based structures

Cite as: AIP Conference Proceedings **1934**, 050002 (2018); <https://doi.org/10.1063/1.5024499>
Published Online: 08 February 2018

O. Oubram, O. Navarro, I. Rodríguez-Vargas, E. J. Guzman, L. Cisneros-Villalobos, and J. G. Velásquez-Aguilar



View Online



Export Citation

ARTICLES YOU MAY BE INTERESTED IN

[Transport properties and thermoelectric effects in gated silicene superlattices](#)
Journal of Applied Physics **124**, 144305 (2018); <https://doi.org/10.1063/1.5045479>

[Silicene: Recent theoretical advances](#)
Applied Physics Reviews **3**, 040802 (2016); <https://doi.org/10.1063/1.4944631>

[Transport properties of silicene-based ferromagnetic-insulator-superconductor junction](#)
Journal of Applied Physics **122**, 043906 (2017); <https://doi.org/10.1063/1.4996347>

AIP | Conference Proceedings

Get **30% off** all
print proceedings!

Enter Promotion Code **PDF30** at checkout



Giant Oscillating Magnetoresistance in Silicene-Based Structures

O. Oubram^{1,a)}, O. Navarro², I. Rodríguez-Vargas^{3,4}, E. J. Guzman^{2,5}, L. Cisneros-Villalobos¹ and J. G. Velásquez-Aguilar¹

¹ *Facultad de Ciencias Químicas e Ingeniería, Universidad Autónoma del Estado de Morelos, Av. Universidad 1001, Col. Chamilpa, 62209 Cuernavaca, Morelos, México.*

² *Unidad Morelia del Instituto de Investigaciones en Materiales, Universidad Nacional Autónoma de México, Antigua Carretera a Pátzcuaro No. 8701, Col. Ex Hacienda de San José de la Huerta, 58190 Morelia, Michoacán, México.*

³ *Unidad Académica de Física, Universidad Autónoma de Zacatecas, Calzada Solidaridad Esquina con Paseo La Bufa s/n, 98060 Zacatecas, Zacatecas, México.*

⁴ *Instituto de Investigaciones en Ciencias Básicas y Aplicadas, Universidad Autónoma del Estado de Morelos, Av. Universidad 1001, Col Chamilpa, 62209, Cuernavaca Morelos, México.*

⁵ *Facultad de Ciencias Físico Matemáticas, Universidad Michoacana de San Nicolás de Hidalgo, Av. Francisco J. Mujica s/n Ciudad Universitaria, Morelia, Michoacán, México.*

a)oubram@uaem.mx

Abstract. Ballistic electron transport in a silicene structure, composed of a pair of magnetic gates, in the ferromagnetic and antiferromagnetic configuration is studied. This theoretical study has been done using the matrix transfer method to calculate the transmission, the conductance for parallel and antiparallel magnetic alignment and the magnetoresistance. Results show that conductance and magnetoresistance oscillate as a function of the length between the two magnetic domains. The forbidden transmission region also increases as a function of the barrier separation distance.

INTRODUCTION

Silicene is a monolayer of silicon atoms, forming a 2D dimensional honeycomb lattice [1]. This new material has attracted more attention due to its special physical properties, similar to those of graphene, as well as for its possible implementation in nanoelectronics [2, 3]. In contrast to graphene, silicene has a large intrinsic spin-orbit interaction and a buckled structure involving valley and spin manipulation [4, 5]. Recently, monolayer and multilayer silicene have been synthesized and a silicene transistor reached [3, 6]. Likewise, D. Wang et al. [7] propose the magnetic field as a tool to manipulate valley and spin transport in silicene. Specifically, They have shown that the conductance and tunneling magnetoresistance (TMR), in a silicene structure with ferromagnetic (FM) barriers, can be controlled by the magnetic field. Furthermore, Y. Wang et al. [2] reported that, in two ferromagnetic barriers on the top of monolayer silicene, the magnetic field affects intensively the transmission of the antiferromagnetic (AFM) configuration of the device and enlarges the forbidden transmission region for the ferromagnetic case. In this work, we explore the ballistic transport in a silicene structure formed by two ferromagnetic strips. We obtain a notable oscillation of the parallel and antiparallel conductance as well as TMR as a function of the separation of the two ferromagnetic strips.

THEORETICAL BACKGROUND

The ferromagnetic junction we are interested in, is a nanodevice that basically consists of a silicene sheet and two ferromagnetic strips with different width d_l and d_r , and separated by a distance L (see Fig. 1). This device has two ferromagnetic configurations, parallel (P) and antiparallel (AP). When, the alignment of the strip of the right side is

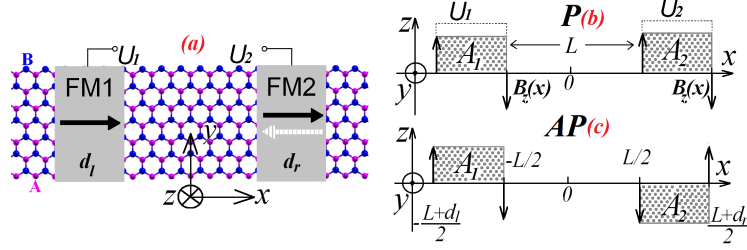


FIGURE 1. (a) Schematic representation of a Ferromagnetic/Normal/Ferromagnetic (FNF) asymmetrical Silicene junction. A typical configuration in such device, consists of two ferromagnetic strips (gray rectangles) deposited on the top of the silicene sheet, separated by a L distance and with different widths (d_l and d_r). Other difference between FM gates, is the magnetization alignment (z -direction), where the right side gate has up or down magnetization. In contrast, the left one is fix. To control the Fermi energy of incident electrons, a local electrostatic potentials and a static magnetic fields are applied on the gates. Parallel (P) (b) and antiparallel (AP) (c) magnetization alignment of FNF silicene junction are induced by a stray field $B_z(x)$. A_1 and A_2 are the corresponding transverse magnetic vector potentials (gray rectangles) for P and AP magnetization alignment. Dashed lines in (b) represents the local electrostatic potentials U_1 and U_2 induced by the top gate voltage.

different to the strip of the left side, the configuration is AP. In contrast, when they have the same alignment it is P (see Fig. 1).

The control of the Fermi energy of the incident electrons is handled by a delta-type magnetic field (z -coordinate) localized in the edges of the FM strips (see Fig. 1) [2, 8]. The magnetic field B_z is formally described in Ref. [2], so, the corresponding magnetic vector potential A is given by $A = [0, A_y(x), 0]$, where $A_y(x)$ is deduced from $A_y(x) = \int_{-\infty}^x B_z(x) dx$ [2]. This FM nanodevice can be described by the low-energy effective Hamiltonian around the Dirac point [9]:

$$H = v_F(\pi_x \tau_x - \eta \pi_y \tau_y) - (\eta \sigma \Gamma_{SO} - \Delta_z) \tau_z + UI, \quad (1)$$

where v_F is the Fermi velocity of the charge carriers in silicene and $\pi_{x(y)} = P_{x(y)} + eA_{x(y)}$ is the canonical momentum with $P_{x(y)}$ the electron momentum. $\tau = (\tau_x, \tau_y, \tau_z)$ corresponds to the sublattice (pseudospin) Pauli matrices, I is the 2×2 unity matrix, $\eta = \pm 1$ denotes the \mathbf{K} and \mathbf{K}' valleys and $\sigma = \pm 1$ denotes the spin indices. Γ_{SO} specifies the spin-orbit coupling, which in silicene has a large value (3.9 meV) [10]. This is a stark difference with respect to graphene. Here, U_1 (U_2) is the height of electrostatic values induced by FM1 (FM2) and Δ_1 (Δ_2) is the on-site potential on the ferromagnetic domain FM1 (FM2) (see Fig. 1).

The corresponding eigenenergy and eigenfunction from Eq. (1) can be straightforwardly deduced as $k_{x,j} = \sqrt{(E - U_j)^2 - (\eta \sigma \Gamma_{SO} - \Delta_{z,j})^2 - (k_{y,j} + A_j)^2}$ and $\psi_j^\pm(x, y) = A_j^\pm \begin{pmatrix} 1 \\ v_j^\pm \end{pmatrix} e^{\pm i k_{x,j} x + i k_{y,j} y}$, j is a specific region.

With the transfer matrix, we can obtain a relation between the coefficients of the forward and backward waves, namely

$$\begin{pmatrix} A_0^+ \\ A_0^- \end{pmatrix} = M \begin{pmatrix} A_{N+1}^+ \\ 0 \end{pmatrix}.$$

Here $j = 1, 2, \dots, N$. In our case $N = 3$. The first, second and third regions for us are the first barrier (FM1), the interwell region and the second barrier (FM2). Knowing the transfer matrix we can calculate easily the tunneling probability, $t_{P/AP}(E, k_y, \eta, \sigma) = \left| \frac{A_{N+1}^+}{A_0^+} \right| = \frac{1}{|M_{11}|}$. With M_{11} being the (1, 1) element of the transfer matrix M . The corresponding ballistic transmission in the silicene sheet for a specific magnetization configuration is $T_{P/AP} = \frac{1}{4} \sum_{\eta=-1}^1 \sum_{\sigma=-1}^1 t_{P/AP}(\eta, \sigma)$. When the transmission probabilities are calculated, the conductance of the system can be obtained through the Landauer-Büttiker formula [11]

$$G_{P/AP}(E_F) = G_0 \int_{-\pi/2}^{\pi/2} T_{P/AP}(E_F, k_F \sin \theta) \cos \theta d\theta, \quad (2)$$

where E_F is the Fermi energy, $G_0 = e^2 L_y k_F / \pi^2 \hbar$ is the fundamental conductance factor with L_y being the width of the system in the transversal y -coordinate, $k_F = \sqrt{E_F^2 - \Gamma_{SO}^2}$ is the Fermi wave-vector and θ is the angle

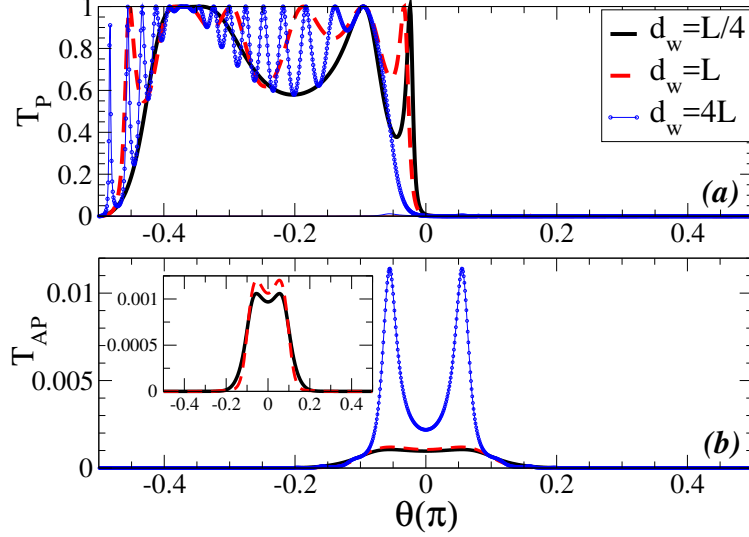


FIGURE 2. (a) Parallel and (b) antiparallel transmission as a function of the incident angle, for different well widths. The solid-black, dashed-red and dotted-blue lines correspond to $d_w = L/4$, $d_w = L$ and $d_w = 4L$ respectively. Here, $U_l = U_r = 2$, $E = 5$, $B_l = B_r = 3$, $\Delta_l = \Delta_r = 0$, and $d_l = d_r = L/2$.

of the incident electrons with respect to the x -coordinate. Thereby, the tunneling magnetoresistance through the Ferromagnetic/Normal/Ferromagnetic (FNF) junction can be defined as $TMR = (G_P - G_{AP})/G_{AP}$.

NUMERICAL AND THEORETICAL RESULTS

We now apply the above formulation to calculate the transmission, conductance and TMR of Dirac fermions in our silicene-based structure. In fact, our structure consists of a quantum well and two ferromagnetic barriers of width d_w and $d_l = d_r$, respectively. We use the following dimensionless parameters, the magnetic field $B = 3$ and a fixed incident energy $E = 5$, with $\Delta_1 = \Delta_2 = 0$ and $U_1 = U_2 = 2$.

In Fig. 2 we display the parallel (a) and the antiparallel (b) transmission probability as a function of the incident angle θ for different separation distances between the barriers, $L/4$, L and $4L$, solid-black, dashed-red and dotted-blue curves, respectively. In Fig. 2a, we notice that more peaks with unitary transmission probability ($T_P = 1$) appear when the separation distance d_w increases. This oscillatory behaviour is due to the resonant tunneling through the barriers. We also notice that the transmission probability for P alignment is completely suppressed for $\theta > 0$, and that the forbidden transmission region increases by increasing d_w . This behavior is explained by the longitudinal momentum k_x in the barrier, which becomes imaginary $k_x = \sqrt{(E - U)^2 - \Gamma_{SO}^2 - (k_y + B)^2}$.

The transmission for the AP alignment is remarkable, since it is strongly suppressed in a wide region (outside the range $\theta_0 < \theta < \theta_1$). Unlike P alignment, the transmission spectrum of AP alignment shows angular isotropy. In this configuration, the magnetic vector $A = -B$ is antisymmetric near the central line $x=0$ and for a given $k_y > 0$ ($k_y < 0$) the appearance of evanescent states in the first barrier FM1 only requires $\sqrt{(E - U)^2 - \Gamma_{SO}^2} < |k_y + B|$ ($\sqrt{(E - U)^2 - \Gamma_{SO}^2} < |-k_y + B|$), whereas in the second barrier FM2, the evanescent states is determined by $\sqrt{(E - U)^2 - \Gamma_{SO}^2} < |k_y - B|$ ($\sqrt{(E - U)^2 - \Gamma_{SO}^2} < |-k_y - B|$). According to the equivalence between k_y and $-k_y$ in the AP configuration for the evanescent states, the transmission spectrum will have symmetric behavior as it is shown in Fig. 1b. Besides, an increasing of transmission probability in Fig. 2b is observed at high d_w distance. This behavior indicates that the decaying length of the evanescent states in FM2 is larger than the barrier width. Moreover, we see that the maximal transmission of T_{AP} is lower than T_P in two orders of magnitude and that the forbidden transmission region has a very large domain. All these features will be exhibited principally in a measurable quantity, the conductance.

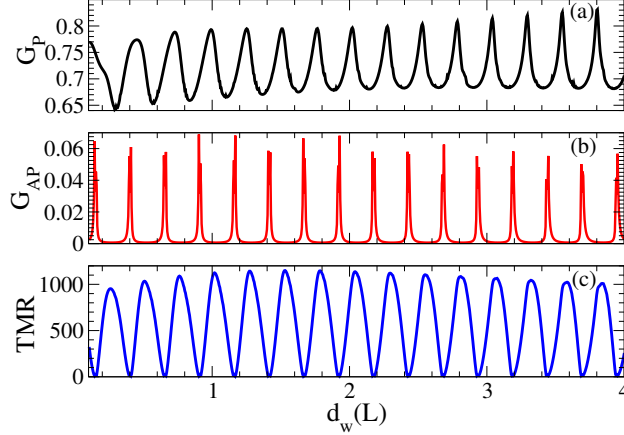


FIGURE 3. (a) Ferromagnetic and (b) antiferromagnetic conductance as well as (c) TMR as a function of d_w . The parameters of the system considered are $d_l = d_r = L$, $B = 3$, $E = 5$ and $\Delta = 0$.

So, to explore the transmission characteristics, we can benefit from the conductance as a measurable property. Then, the conductance is a valuable experimental property to analyse the electron transport properties of the system. The conductance for P and AP alignment and TMR as function of d_w are shown in Fig.3a, b and c, respectively. As we can notice the conductance presents an oscillatory behavior for both magnetic configurations, parallel and antiparallel. This behavior is related to the interference conditions that take place between the reflected and incident electrons in the non-ferromagnetic region [12]. On the other hand, the conductance changes with d_w in oscillatory fashion due to the Klein tunneling of Dirac fermions [7]. Indeed, Klein tunneling is significant in the P configuration, nearly 65% of the conductance. In contrast, it is lower than 65×10^{-2} for the AP configuration due to the low transmission probability with respect to angle of incidence. Furthermore, this oscillatory behavior, of both configurations, will be present in TMR, see Fig. 3c. As we can see the maximum of TMR is located in regions of low G_{AP} (regions of high G_P) as a result of the intensive suppression of transmission in the AP alignment and the strong manifestation of the transmission in the P alignment.

In summary, we have investigated the ballistic transport in double magnetic barriers in silicene. We have shown that the conductance in the ferromagnetic and antiferromagnetic configuration as well as the tunneling magnetoresistance oscillate as a functions of the distance separation between barriers.

ACKNOWLEDGMENTS

This work was supported by PRODEP-SEP Program and partially supported by PAPIIT-IN104616 from UNAM.

REFERENCES

- [1] K. Takeda and K. Shiraishi, *Phys. Rev. B* **50**, 14916 (1994).
- [2] Y. Wang, Y. Lou, *J. Appl. Phys.* **114**, 183712 (2013).
- [3] L. Tao, et al. *Nature Nanotech.* **10**, 227 (2015).
- [4] X.L. Qi, S.-C. Zhang, *Phys. Today*, **63**, 33 (2010).
- [5] N. D. Drummond, V. Zólyomi, V. I. Fal'ko, *Phys. Rev. B* **85**, 075423 (2012).
- [6] P. Vogt et al. *Phys. Rev. Lett.* **108**, 155501 (2012).
- [7] D. Wang, Z. Huang, Y. Zhang, G. Jin, *Phys. Rev. B* **93**, 195425 (2016).
- [8] F. Zhai, K. Chang, *Phys. Rev. B* **77**, 113409 (2008).
- [9] T. Yokoyama, *Phys. Rev. B* **87**, 241409R (2013).
- [10] C. C. Liu, H. Jiang, and Y. G. Yao, *Phys. Rev. B* **84**, 195430 (2011).
- [11] S. Datta, *Electronic Transport in Mesoscopic Systems*, Cambridge University Press, 1995.
- [12] X. J. Qiu, Y. F. Cheng, Z. Z. Cao, J. M. Lei, *J. Phys. D: Appl. Phys.* **48** 465105 (2015).